

A Simplified Model for Predicting and Designing High-Temperature Ambient-Pressure Superconductors

Yuting Sun^{1#}, Shixu Liu^{1#}, Xin-Gao Gong^{1*}, and Ji-Hui Yang^{1*}

¹Key Laboratory for Computational Physical Sciences (MOE), State Key Laboratory of Surface Physics, Department of Physics, Fudan University, Shanghai 200433, China

[*corresponding authors](#)

[Email: xggong@fudan.edu.cn](mailto:xggong@fudan.edu.cn); jhyang04@fudan.edu.cn

[#These authors contribute equally to this work.](#)

ABSTRACT:

Searching for ambient-pressure conventional superconductors with critical temperatures (T_C) higher than 40 K and implementable synthesis routes is a key challenge in the field of high-temperature superconductivity, mainly due to lack of efficient and effective models to estimate T_C of potential systems. In this work, we propose a simplified model to estimate the dimensionless electron-phonon coupling (EPC) strength λ and thus T_C by separately treating the EPC matrix elements which evaluate the pairing strength and the phonon-assisted nesting function $P(\omega)$ which evaluates the matching of electron bands and phonon spectra for forming potential electron pairs via phonons. By applying the model to screen over the Computational 2D Materials Database (C2DB), we successfully identify several systems with T_C exceeding 20 K as confirmed by accurate first-principles calculations. Especially, $Ti_3N_2H_2$ has a record high T_C value among known MXenes, which is 52 K (78 K) according to isotropic (anisotropic) Migdal-Eliashberg equations under ambient pressure. More importantly, we propose a feasible synthesis route for $Ti_3N_2H_2$ starting from the experimentally synthesized MXene Ti_4N_3 . Beyond demonstrating its feasibility and efficiency in identifying high- T_C superconductors, our model illuminates the critical roles of the matching between electron band and phonon spectra as a necessary condition in determining T_C and points out the directions for prediction and design of high- T_C superconductors, which is exemplified by showing a novel designed system $Ti_2ScN_2H_2$ with a possible T_C of 80 K under ambient pressure. Our model opens new avenues for exploring high- T_C systems.

KEYWORDS:

Superconductivity, ambient-pressure superconductors, phonon-assisted nesting function, materials prediction and design, $Ti_3N_2H_2$

Superconductivity has been a highly prominent and intensely studied topic since its first discovery in mercury back to 1911 [1]. Despite more than a century of effort, superconductors with high T_C at ambient pressure are still very rare in the field of condensed matter physics. So far, ambient-pressure superconductors with T_C above 40 K are only limited to unconventional superconductors including copper oxides [2-4] and some iron-based compounds [5] while the record T_C of conventional superconductors is only 39 K, which was reported in MgB_2 in 2001 [6]. Note that, they are all first discovered by experiments without exceptions. Theoretically, because the mechanisms for unconventional superconductors are still unclear and thus reliable predictions are quite lacking, intensive efforts have been devoted to searching for conventional superconductors, which can be well explained by the Bardeen-Cooper-Schrieffer (BCS) theory [7,8] and accurately predicted by the Eliashberg methods [9,10]. Great success has been achieved by predicting high- T_C hydride compounds such as SH_3 [11], LaH_{10} [12], and CaH_6 [13] under extremely high pressures, which were later confirmed by experiments [14,15]. Meanwhile, several systems are predicted to have T_C above 40 K at ambient pressure, such as Al_4H (54 K [16]), $(Be_4)_2H$ (72-84 K [17]), hydrogenated monolayer MgB_2 (67 K [18]), LiB_2C_2 trilayer films (92 K [19]), $Li_3B_4C_2$ (54 K [20]) and Mg_2XH_6 ($X= Rh, Ir, Pd, \text{ or } Pt$) (45-160 K [21,22]). However, these materials are generally difficult to be realized experimentally either due to lack of feasible routes or requirement of a plausible high-pressure synthesis process. Consequently, high-temperature ambient-pressure conventional superconductors that are more readily implementable are still under urgent exploration.

The prevailing and most commonly used method for predicting superconductors is to calculate T_C by solving the Eliashberg equations, which is, however, very challenging for material screening due to heavy computational cost. Therefore, some preliminary evaluations have to be made to substantially attenuate computational complexity. It's generally accepted that systems with high density of states (DOS) at the Fermi surface $N(0)$ and high phonon frequency or Debye temperature θ_D tend to have high T_C [23-25]. Actually, current high-throughput screenings of high- T_C BCS superconductors using density functional theory (DFT) calculations and machine learning methods do often use these fundamental parameters in their models [23,24,26]. Some works also consider estimated EPC strength [27,28] in order to make accurate predictions. Besides, large Fermi surface nesting is also thought as possible indications of high T_C [29]. Despite the significant advances in the search for superconductors, the development of an efficient model for the

preliminary screening of high-temperature ambient-pressure conventional superconductors remains an unmet challenge, limiting the pace of discovery in this critical field.

In this work, we first derive a simplified model to estimate the dimensionless EPC strength λ to accelerate the search of high- T_C superconductors. Within the Migdal-Eliashberg theory framework, the isotropic Eliashberg spectral function for phonon energy ω is given by [9,10,30]:

$$\alpha^2 F(\omega) = \frac{1}{2N(0)} \sum_{m\nu\mathbf{k}\mathbf{q}} |g_{m\nu}(\mathbf{k}, \mathbf{q})|^2 \delta(\varepsilon_{n\mathbf{k}} - \varepsilon_F) \delta(\varepsilon_{m\mathbf{k}+\mathbf{q}} - \varepsilon_F) \delta(\omega - \omega_{\mathbf{q}\nu}) \quad (1),$$

where $\varepsilon_{n\mathbf{k}}$ and $\varepsilon_{m\mathbf{k}+\mathbf{q}}$ are the eigenvalues for the Kohn-Sham states, while ε_F refers to the Fermi energy. $\omega_{\mathbf{q}\nu}$ represents the frequency of phonon mode $\mathbf{q}\nu$. $g_{m\nu}(\mathbf{k}, \mathbf{q})$ is the corresponding EPC matrix element. The dimensionless EPC strength λ is then expressed as [31,32]:

$$\begin{aligned} \lambda &= 2 \int_0^\infty \frac{\alpha^2 F(\omega)}{\omega} d\omega \\ &= \int_0^\infty \frac{1}{N(0)} \sum_{m\nu\mathbf{k}\mathbf{q}} \frac{1}{\omega} |g_{m\nu}(\mathbf{k}, \mathbf{q})|^2 \delta(\varepsilon_{n\mathbf{k}} - \varepsilon_F) \delta(\varepsilon_{m\mathbf{k}+\mathbf{q}} - \varepsilon_F) \delta(\omega - \omega_{\mathbf{q}\nu}) d\omega \\ &= \int_0^\infty \frac{\partial \lambda}{\partial \omega} d\omega \end{aligned} \quad (2).$$

Here,

$$\frac{\partial \lambda}{\partial \omega} = \frac{1}{N(0)} \sum_{m\nu\mathbf{k}\mathbf{q}} \frac{1}{\omega} |g_{m\nu}(\mathbf{k}, \mathbf{q})|^2 \delta(\varepsilon_{n\mathbf{k}} - \varepsilon_F) \delta(\varepsilon_{m\mathbf{k}+\mathbf{q}} - \varepsilon_F) \delta(\omega - \omega_{\mathbf{q}\nu}) \quad (3)$$

can be seen as the phonon-energy resolved dimensionless EPC strength. It is well known that, to get accurate converged results of λ and thus superconductivity, the EPC matrix elements on very dense \mathbf{k} and \mathbf{q} grids must be obtained, which would require very expensive computational costs, thus hindering the efficient prediction of high- T_C superconductors. To avoid the direct EPC calculations, here we decompose $\frac{\partial \lambda}{\partial \omega}$ into two separate terms by omitting the wavevector-dependence of g , i.e.:

$$\frac{\partial \lambda}{\partial \omega} = |g^*(\omega)|^2 P(\omega) \quad (4),$$

where $g^*(\omega)$ can be seen as the phonon-energy resolved and wavevector-averaged EPC matrix element. $P(\omega)$ is expressed as:

$$P(\omega) = \frac{1}{N(0)} \sum_{m\nu\mathbf{k}\mathbf{q}} \frac{1}{\omega} \delta(\varepsilon_{n\mathbf{k}} - \varepsilon_F) \delta(\varepsilon_{m\mathbf{k}+\mathbf{q}} - \varepsilon_F) \delta(\omega - \omega_{\mathbf{q}\nu}) \quad (5),$$

which denotes the pairing potentiality of two electrons with energies of $\varepsilon_{n\mathbf{k}}$ and $\varepsilon_{m\mathbf{k}+\mathbf{q}}$ with the help of a phonon with energy of ω . Compared to the Fermi surface nesting function, $P(\omega)$ has an extra $\delta(\omega - \omega_{\mathbf{qv}})$ term which specifically includes roles of phonons. Therefore, we name $P(\omega)$ as phonon-assisted nesting function which can be easily and accurately calculated from the band structure and phonon spectrum. Note that, a larger integration of $P(\omega)$ over ω , i.e., $P = \int P(\omega) d\omega$, indicates that more electrons could form pairs via phonons and therefore a potentially higher T_C . Considering that, larger systems, such as supercells, typically contain more electrons per cell, it is more appropriate to normalize P , i.e., by dividing it by the total atomic mass M of the cell.

As for the $g^*(\omega)$ term, although it is difficult to get accurate results without performing first-principles calculations, some knowledge learned from previous studies can still be borrowed. For example, it is known that there is isotope effect in BCS superconductors which suggests if the element involved in forming Cooper pairs has larger atomic mass m^* (typically the element has significant contributions to the electronic density of states at the Fermi level), it often leads to smaller EPC, i.e.:

$$|g^*(\omega)|^2 \propto \frac{1}{m^*} \quad (6).$$

Combining Eqs. (5) and (6), we can generally use $\frac{P}{m^*M}$ as a descriptor for the preliminary screening of large λ and thus high T_C . Details can be found in the Supplemental Materials (SM).

Once λ is known, according to the Allen-Dynes-modified McMillan formula, T_C can be approximated by the following equation [31,32]:

$$T_C = \frac{\omega_{\log}}{1.2} \exp \left[-\frac{1.04(1 + \lambda)}{\lambda - \mu_c^*(1 + 0.62\lambda)} \right] \quad (7),$$

where μ_c^* is the Coulomb pseudopotential with values ranging from 0.1 to 0.2. ω_{\log} is logarithmic average of phonon frequencies and can be calculated as:

$$\begin{aligned} \omega_{\log} &= \exp \left[\frac{2}{\lambda} \int_0^\infty \frac{\alpha^2 F(\omega)}{\omega} \log(\omega) d\omega \right] \\ &= \exp \left[\frac{1}{\lambda} \int_0^\infty |g^*(\omega)|^2 P(\omega) \log(\omega) d\omega \right] \end{aligned} \quad (8).$$

Furthermore, for an ideal model system with just one flat optical phonon branch with a constant frequency of ω_{LO} , λ can be further simplified as $\frac{CN(0)}{m^*M\omega_{LO}}$ where C is a fitting constant, and ω_{\log} is

just equal to ω_{LO} . In this case, even T_C can be quickly estimated without knowing the band structure and phonon spectrum, making it especially useful for efficient preliminary screenings of high T_C systems (see details in SM).

We then apply the above model to search for high- T_C ambient-pressure superconductors. Here we choose the C2DB [33,34] for high-throughput screening because it contains information of phonon frequencies for many metallic systems. The workflow is shown in Fig. 1a. The starting point is the 16789 monolayer materials currently available in C2DB. In the first step, we select the materials that meet the criteria of metallic behavior, dynamic stability, and non-magnetism, resulting in 1036 candidates. Next, considering the fact that low frequency will limit ω_{log} and thus T_C , we require the maximum phonon frequency ω_{max} larger than 42 meV considering that the exponential term in Eq. 7 is usually no larger than 0.1~0.15 at ambient pressure, resulting in 576 candidates. Then, because the lacking of the phonon spectra for many systems and heavy computational cost to accurately calculate them, we do preliminary screenings by using our model considering just ω_{LO} , $N(0)$ and atomic masses, i.e., $\lambda = \frac{CN(0)}{m^*M\omega_{LO}}$ and $\omega_{log} = \omega_{LO}$, identifying 108 materials with estimated T_C exceeding 35 K (see Fig. 1b and SM). Subsequently, we conduct first-principles calculations of phonon spectra to obtain accurate $P(\omega)$ and P . The systems with imaginary phonon modes are spontaneously discarded. As discussed above, larger $\frac{P}{m^*M}$ indicates larger λ . To further narrow the number of ideal candidates, we also consider that, if P has a larger portion in the high- ω region, more optical phonon modes will be involved in forming Cooper pairs and thus leading to larger ω_{log} . Therefore, we would expect the systems lying in the top right corner of Fig. 1c tend to have high T_C . Finally, we use the EPW code [35-37] to accurately calculate their superconductivity properties. Our first-principles calculations are performed by using the Quantum Espresso Package [38,39] with the norm-conserving pseudopotentials [40]. All 2D metals are described using a vacuum-slab model and the 2D Coulomb cutoff approach [41] is used. More first-principles calculation details can be found in the SM.

After performing the above high-throughput screening process, we successfully identify 6 systems with T_C higher than 20 K according to accurate first-principles calculations. Their structures and T_C values are shown in the inset of Fig. 1c. Among them, we find that $Ti_3N_2H_2$ has a T_C value of 52 K (78 K) by solving the isotropic (fully anisotropic) Migdal-Eliashberg equations on an interpolated k-point grid of $600 \times 600 \times 1$ ($300 \times 300 \times 1$) and a q-point grid of $200 \times 200 \times 1$

(100×100×1). Thorough convergence tests are carefully conducted with details provided in the SM. In the following, we just focus on $\text{Ti}_3\text{N}_2\text{H}_2$ in the main text and the detailed superconductivity properties of other systems can be found in the SM.

As seen in Fig. 2a, $\text{Ti}_3\text{N}_2\text{H}_2$ exhibits the characteristic hydrogenated MXene structure, consisting of nitrogen layers sandwiched between two Ti layers with H atoms directly bonded to the outmost Ti atoms. Currently, a significant amount of research has been conducted on the superconductivity of MXenes [42] and reported the crucial role of surface functionalization in enhancing T_C . For instance, non-superconducting Nb_2C can achieve a T_C of 14.4 K if functionalized with O [43]. Hydrogenated Mo_2N and 1T- Mo_2NC_2 exhibit notable T_C of 32.4 K and 42.7 K respectively [44,45]. Among all known MXenes, we find that $\text{Ti}_3\text{N}_2\text{H}_2$ has the highest T_C reported to date as far as we know.

What is more important is that, MXenes have well-established preparation methods with more than 50 systems synthesized experimentally [46]. Among them, Ti_4N_3 featuring four layers of Ti separated by three layers of N is successfully fabricated in 2016 [47]. If the top TiN layer is exfoliated, Ti_3N_2 can then be made. Our calculated exfoliation energy is $73 \text{ meV}/\text{\AA}^2$, which, compared to the successful synthesis of 2D SnSe [48,49] with an exfoliation energy close to $89 \text{ meV}/\text{\AA}^2$ [50] and hematene [51] with a surprisingly high exfoliation energy of $140 \text{ meV}/\text{\AA}^2$ [52,53], indicates the relatively easy formation of Ti_3N_2 . Then $\text{Ti}_3\text{N}_2\text{H}_2$ can be obtained by hydrogenation, which is also energetically favorable as this process is exothermic with an energy release of 2.53 eV per formula. We further performed molecular dynamics (MD) simulations and found that hydrogen keeps bonded to Ti even at $T=600 \text{ K}$, indicating the robust thermodynamic stability of $\text{Ti}_3\text{N}_2\text{H}_2$ (see SM). Based on the above discussions, the experimental realization of $\text{Ti}_3\text{N}_2\text{H}_2$ is sufficiently expected.

To uncover the reason for the exceptionally high T_C in $\text{Ti}_3\text{N}_2\text{H}_2$, we conduct a systematic investigation of its electronic structure properties. Fig. 2b shows the band structure of $\text{Ti}_3\text{N}_2\text{H}_2$ using the local density approximation (LDA) functional [54]. As can be seen, there are two energy bands crossing the Fermi level with one band that lies exactly at the Fermi level rather flat along the M- Γ line and near the K point. Consequently, $N(0)$ has a relatively large value of 11.2 states/eV. Total DOS (TDOS) calculations show that $N(0)$ is mainly contributed by Ti1 and Ti2 atoms with partial contributions from N atoms (see Fig. 2c), while the middle Ti layer has negligible contributions. Orbital-projected DOS (PDOS) in Fig. 2d indicates that $N(0)$ is constituent of Ti

d orbitals and N p_z orbitals, indicating relatively strong p-d hybridizations. Note that, if the Fermi level is shifted downward upon hole doping which could happen if the hydrogenation is not fully saturated, $N(0)$ can be further increased. We have also tested the Perdew-Burke-Ernzerhof (PBE) [55] functionals, finding the similar characters of band structures (see SM). In the followings, we mainly present the LDA results while the PBE results are provided in the SM which yield similar results.

The calculated vibrational spectrum in the harmonic approximation is shown in Fig. 3a. The absence of imaginary phonon modes indicates its dynamical stability. Interestingly, the vibration modes of $\text{Ti}_3\text{N}_2\text{H}_2$ can be divided into three distinct regions, that is, the low-phonon-energy region ($0 < \omega < 45$ meV), the medium-phonon-energy region ($60 < \omega < 75$ meV), and the high-phonon-energy region ($110 < \omega < 130$ meV), which are predominantly contributed by the vibrations of Ti, N, and H atoms, respectively, as shown in Fig. 3b. This character might be due to the localization of phonon modes. The consequence is that, the individual contributions to the total λ from each type of atom are also easily distinguished. Fig. 3c shows the isotropic Eliashberg spectral function $\alpha^2F(\omega)$, and the cumulative electron-phonon coupling parameter $\lambda(\omega)$, obtained by integrating $2\alpha^2F(\omega)/\omega$ over ω . It is clearly seen that Ti, N and H contribute 64%, 33%, and 3%, respectively, to the total λ , corresponding to the three jumps of $\lambda(\omega)$ in the low-, medium-, and high-phonon-energy regions. Our calculated total λ is 1.5 and ω_{\log} is 38 meV, yielding a T_C of 52 K assuming $\mu_c^* = 0.1$ within the isotropic Eliashberg framework. Note that, T_C can reach about 65 K if considering the strong coupling and shape corrections or 78 K if solving the fully anisotropic Migdal-Eliashberg equations (see SM).

To elucidate the origin of remarkable superconductivity properties of $\text{Ti}_3\text{N}_2\text{H}_2$ and demonstrate the important role of $P(\omega)$ in assessing the pairing potentiality of two electrons via phonons, we make a comparative study with bulk MgB_2 . Fig. 4 gives the $\frac{\partial\lambda}{\partial\omega}$, $P(\omega)$, and $|g^*(\omega)|^2$ of $\text{Ti}_3\text{N}_2\text{H}_2$ and MgB_2 . As we can see that, $\text{Ti}_3\text{N}_2\text{H}_2$ has a much larger λ than MgB_2 . Detailed analysis shows that, on the one hand, $P(\omega)$ of $\text{Ti}_3\text{N}_2\text{H}_2$ as well as integrated $P(\omega)$ is 20~30 times higher than that of MgB_2 , indicating that the matching of electron bands and phonon spectra in $\text{Ti}_3\text{N}_2\text{H}_2$ is much better for the potential formation of Cooper pairs. This can be attributed to two reasons. First, $N(0)$ is significantly higher in $\text{Ti}_3\text{N}_2\text{H}_2$ and thus there are more electrons ready to pair. Second, there are more soft phonons in $\text{Ti}_3\text{N}_2\text{H}_2$ due to the heavier Ti and N atoms, which favors the matching

between the electronic band structure and the phonon spectrum for facilitating superconducting pairing. On the other hand, the pairing strength $|g^*(\omega)|^2$ is about one order of magnitude smaller in $\text{Ti}_3\text{N}_2\text{H}_2$, which can be attributed to the relatively weak electron-phonon couplings due to heavier Ti and N atoms. Nevertheless, the tremendously large $P(\omega)$ in $\text{Ti}_3\text{N}_2\text{H}_2$ dominates over the pairing strength, leading to the larger λ , justifying the use of $P(\omega)$ for searching for high- T_C superconductors.

Another interesting finding is that, the peaks of $P(\omega)$ and $|g^*(\omega)|^2$ are well matched in $\text{Ti}_3\text{N}_2\text{H}_2$ while they are mismatched in MgB_2 . If MgB_2 can be engineered to have better matching between its electronic band structure and phonon spectrum, a much more enhanced T_C could be expected. Taking H- MgB_2 [18] as an illustrative case, its integrated $P(\omega)$ value is several times greater than that of MgB_2 . Additionally, H- MgB_2 exhibits enhanced peaks of $|g^*(\omega)|^2$ in the low- ω region, demonstrating better alignment with its $P(\omega)$. These two factors culminate in a substantially higher T_C in H- MgB_2 (see SM). Similarly, T_C of $\text{Ti}_3\text{N}_2\text{H}_2$ can also be increased by the further improvement of $P(\omega)$. We note that, $\text{Ti}_3\text{N}_2\text{H}_2$ has a more pronounced peak in the DOS lying at about 0.2 eV below the Fermi level. If the Fermi level can be shifted downward by hole doping, a larger $N(0)$ and thus larger $P(\omega)$ would be expected. Indeed, we find that this can be realized by replacing the middle Ti layer with Sc layer. Note that, the middle metal layer has negligible contribution to the states near the Fermi level (see Fig. 2c), so the newly designed $\text{Ti}_2\text{ScN}_2\text{H}_2$ system has similar band characters with $\text{Ti}_3\text{N}_2\text{H}_2$ except that it has more electrons ready to pair. Consequently, $\text{Ti}_2\text{ScN}_2\text{H}_2$ has even larger $P(\omega)$ and thus higher T_C . Our calculations show that $\text{Ti}_2\text{ScN}_2\text{H}_2$ remains dynamically stable and demonstrates remarkable superconductivity, with T_C reaching 54 K and 80 K by rigorous calculations employing isotropic and anisotropic Migdal-Eliashberg theoretical frameworks, respectively (see SM).

Finally, using our proposed model, we can also understand why high- T_C BCS superconductors are often theoretically reported in 2D or layered systems. Generally speaking, on the one hand, 2D metals will have larger electron and phonon density of states due to quantum confinement effects [56]. Therefore, electrons have a larger chance to form pairs via phonons, that is, $P(\omega)$ tends to be larger in 2D. On the other hand, due to the reduced dimension, the screening effects are suppressed. Consequently, the pairing strength $|g^*(\omega)|^2$ will be increased. These two characters of 2D metals will help obtaining larger λ , resulting in high T_C .

In summary, we have derived a simplified model to estimate the dimensionless EPC strength λ by separately treating the EPC matrix elements which evaluate the pairing strength and the phonon-assisted nesting function $P(\omega)$ which evaluates potentiality of electron pairing via phonons, thereby greatly accelerating the search of high- T_C superconductors. By applying the model in a high-throughput workflow, we have identified high- T_C ambient-pressure superconducting systems. Among them, we have found that $Ti_3N_2H_2$ have record-high T_C of 52 K among known MXenes due to its extremely large $P(\omega)$ values. We have also proposed experimental synthesis route of $Ti_3N_2H_2$ and thus experimental works are strongly called for. Furthermore, we have shown that, our model can also help guiding the design of high- T_C superconductors by proposing a new MXene system $Ti_2ScN_2H_2$, which can have a T_C of as high as 80 K due to the increased $P(\omega)$. Besides, we have explained why high- T_C superconductors are often predicted in 2D systems using our model. We expect our work will help to find more high- T_C ambient-pressure superconductors in the future.

ACKNOWLEDGMENTS

This work was partially supported by the China National Key R&D Program (2022YFA1404603), the National Natural Science Foundation of China (Grants No. 12188101, No.11991061 and No. 12474222), the ShanghaiPilot Program for Basic Research-FuDan University 21TQ1400100(22TQ017), and the Guangdong Major Project of the Basic and Applied Basic Research (Future functional materials under extreme conditions 2021B0301030005).

FIGURES

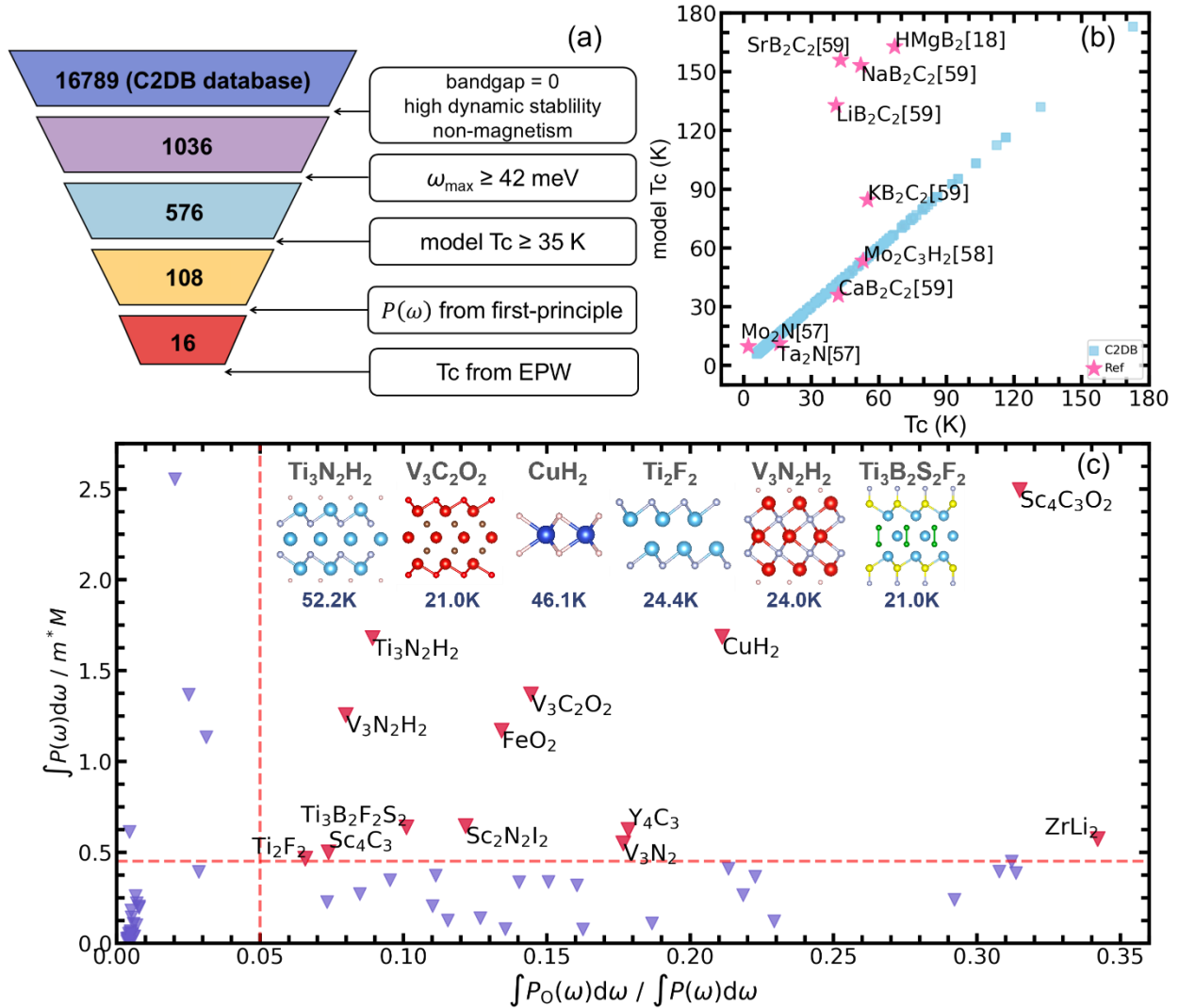


Fig. 1. Schematics illustrating the screening process of identifying high-temperature ambient-pressure 2D superconductors. (a) An illustration of preliminary high-throughput workflow applied C2DB database. The screening criteria and number of materials at each step of the workflow are given. (b) Model T_c obtained from $\lambda = \frac{CN(0)}{m^*M\omega_{LO}}$ and $\omega_{\log} = \omega_{LO}$ for preliminary screenings. Here C is a fitting constant obtained from known systems denoted as pink stars [18,57-59]. Blue square markers, with their abscissas and ordinates representing T_c predicted by the model for metallic materials from C2DB database, delineate the $y = x$ identity line. (c) Fine screening of candidate materials based on $\frac{P}{m^*M}$ and portion of P in the high- ω region denoted as P_O , both obtained from first-principles calculations of electron structures and phonon spectra. Two red lines oriented

perpendicular and parallel to the x-axis represent threshold values slightly exceeding those computed for MgB₂.

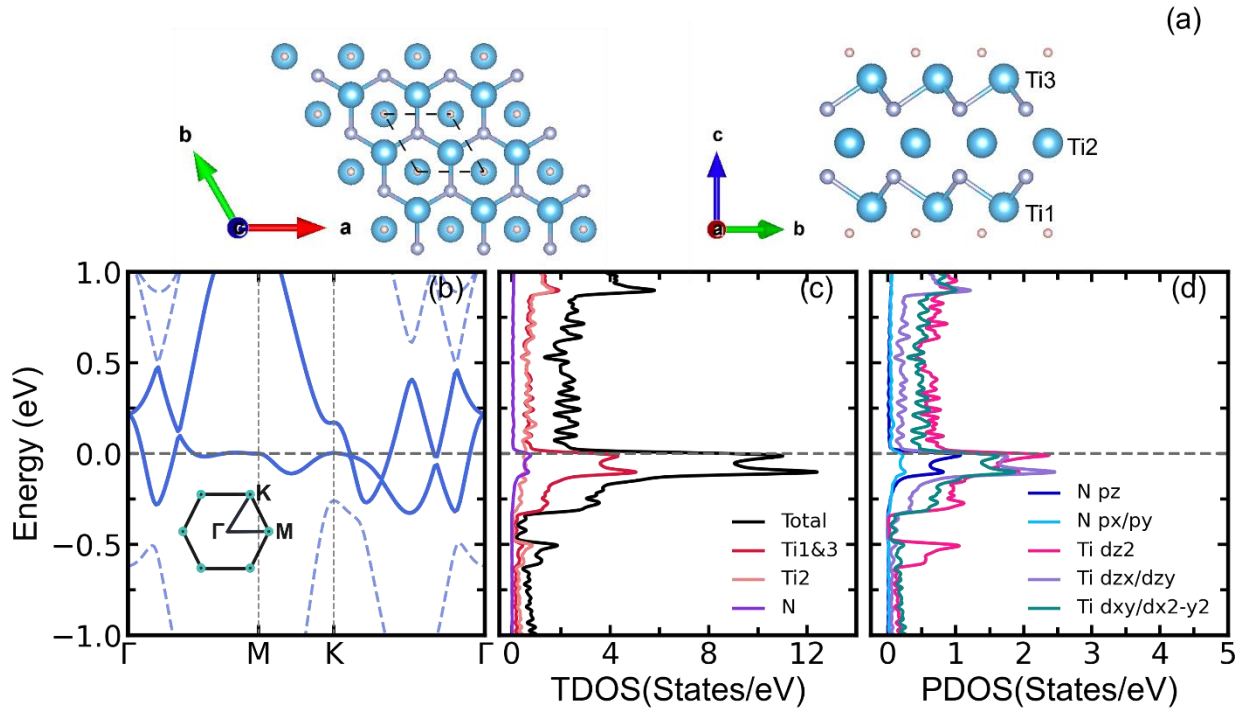


Fig. 2. Structures and electronic structures of $\text{Ti}_3\text{N}_2\text{H}_2$. (a) Top and side views of $\text{Ti}_3\text{N}_2\text{H}_2$ monolayer. Titanium, nitrogen and hydrogen atoms are represented by blue, purple and pink spheres, respectively. (b) Electronic band structure of $\text{Ti}_3\text{N}_2\text{H}_2$ along high-symmetry line Γ -M-K- Γ . The Fermi level indicated by the dotted line is set to 0 eV. (c) The total DOS (TDOS) of $\text{Ti}_3\text{N}_2\text{H}_2$ contributions of Ti, N and H atoms. (d) The partial density of states (PDOS) of $\text{Ti}_3\text{N}_2\text{H}_2$.

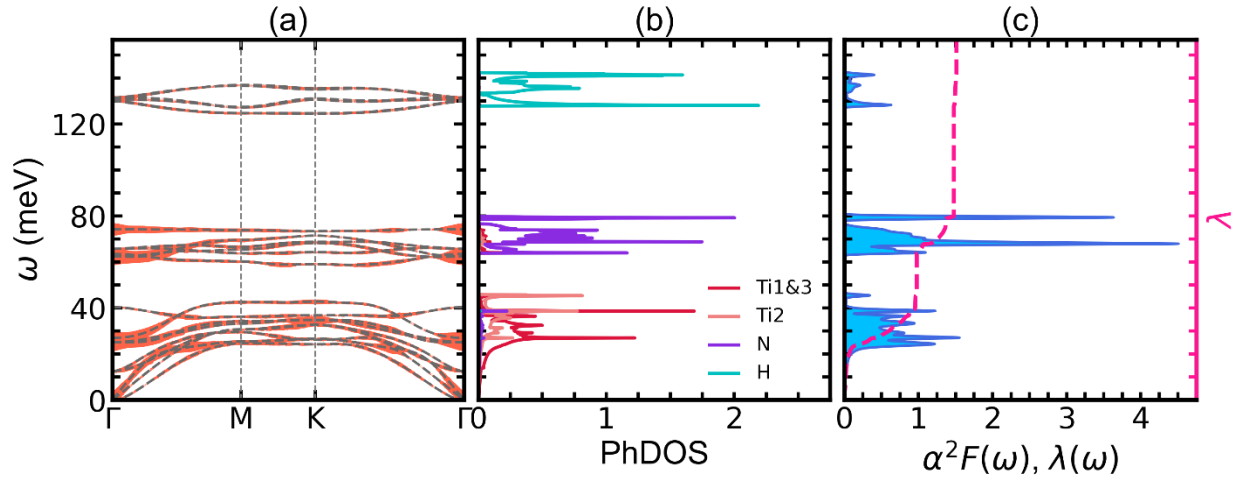


Fig. 3. Vibrational and superconducting properties of $\text{Ti}_3\text{N}_2\text{H}_2$. (a) Phonon dispersion of $\text{Ti}_3\text{N}_2\text{H}_2$ weighted by the magnitude of the EPC constant $\lambda_{\mathbf{q}\nu}$ for phonon mode $\mathbf{q}\nu$. (b) The atomic projected phonon DOS. (c) Eliashberg spectral function $\alpha^2 F(\omega)$ and cumulative electron-phonon coupling parameter $\lambda(\omega)$.

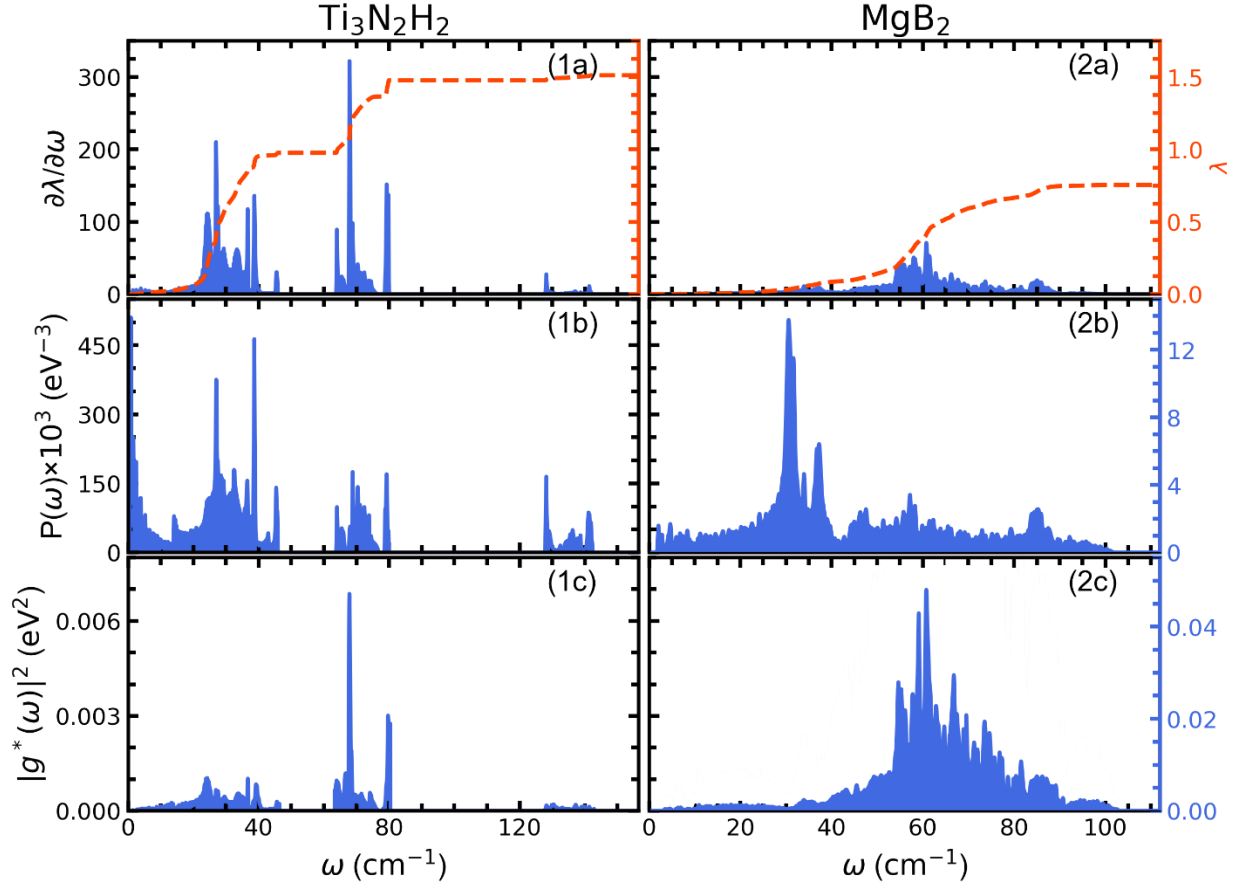


Fig. 4. Comparisons of superconductivity properties of $\text{Ti}_3\text{N}_2\text{H}_2$ and MgB_2 . (a) The phonon-energy resolved dimensionless EPC strength $\frac{\partial\lambda}{\partial\omega}$, (b) phonon-assisted nesting function, and (c) averaged electron-phonon coupling $|g^*(\omega)|^2$ in $\text{Ti}_3\text{N}_2\text{H}_2$ and MgB_2 . The red lines in the top panels indicate the integrated $\frac{\partial\lambda}{\partial\omega}$ over ω , which is also equal to $\lambda(\omega)$ in Fig. 3c.

REFERENCE

- [1] H. K. Onnes, *Comm. Phys. Lab. Univ. Leiden* **122**, 124 (1911).
- [2] Y. Tokura, H. Takagi, and S. Uchida, *Nature* **337**, 345 (1989).
- [3] A. Gozar, G. Logvenov, L. F. Kourkoutis, A. Bollinger, L. Giannuzzi, D. Muller, and I. Bozovic, *Nature* **455**, 782 (2008).
- [4] G. Logvenov, A. Gozar, and I. Bozovic, *Science* **326**, 699 (2009).
- [5] H. Hosono and K. Kuroki, *Physica C: Superconductivity and its Applications* **514**, 399 (2015).
- [6] J. Nagamatsu, N. Nakagawa, T. Muranaka, Y. Zenitani, and J. Akimitsu, *nature* **410**, 63 (2001).
- [7] J. Bardeen, L. N. Cooper, and J. R. Schrieffer, *Physical review* **108**, 1175 (1957).
- [8] J. Bardeen, L. N. Cooper, and J. R. Schrieffer, *Physical Review* **106**, 162 (1957).
- [9] A. Migdal, *Sov. Phys. JETP* **7**, 996 (1958).
- [10] G. Eliashberg, *Sov. Phys. JETP* **11**, 696 (1960).
- [11] A. Drozdov, M. Eremets, I. Troyan, V. Ksenofontov, and S. I. Shylin, *Nature* **525**, 73 (2015).
- [12] M. Somayazulu, M. Ahart, A. K. Mishra, Z. M. Geballe, M. Baldini, Y. Meng, V. V. Struzhkin, and R. J. Hemley, *Physical review letters* **122**, 027001 (2019).
- [13] H. Wang, J. S. Tse, K. Tanaka, T. Iitaka, and Y. Ma, *Proceedings of the National Academy of Sciences* **109**, 6463 (2012).
- [14] A. Drozdov *et al.*, *Nature* **569**, 528 (2019).
- [15] L. Ma *et al.*, *Physical Review Letters* **128**, 167001 (2022).
- [16] Y. He, J. Lu, X. Wang, and J.-j. Shi, *Physical Review B* **108**, 054515 (2023).
- [17] Y. He and J.-j. Shi, *Nano Letters* **23**, 8126 (2023).
- [18] J. Bekaert, M. Petrov, A. Aperis, P. M. Oppeneer, and M. Milošević, *Physical review letters* **123**, 077001 (2019).
- [19] M. Gao, X.-W. Yan, Z.-Y. Lu, and T. Xiang, *Physical Review B* **101**, 094501 (2020).
- [20] M. Gao, Z.-Y. Lu, and T. Xiang, *Physical Review B* **91**, 045132 (2015).
- [21] K. Dolui, L. J. Conway, C. Heil, T. A. Strobel, R. P. Prasankumar, and C. J. Pickard, *Physical Review Letters* **132**, 166001 (2024).
- [22] A. Sanna, T. F. Cerqueira, Y.-W. Fang, I. Errea, A. Ludwig, and M. A. Marques, *npj Computational Materials* **10**, 44 (2024).
- [23] D. Wines, K. Choudhary, A. J. Biacchi, K. F. Garrity, and F. Tavazza, *Nano letters* **23**, 969 (2023).

- [24] A. D. Smith, S. B. Harris, R. P. Camata, D. Yan, and C.-C. Chen, *Physical Review B* **108**, 174514 (2023).
- [25] I. Esterlis, S. Kivelson, and D. Scalapino, *npj Quantum Materials* **3**, 59 (2018).
- [26] S. Xie *et al.*, *npj Computational Materials* **8**, 14 (2022).
- [27] A. M. Shipley, M. J. Hutcheon, R. J. Needs, and C. J. Pickard, *Physical Review B* **104**, 054501 (2021).
- [28] G. D. Gaspari and B. L. Gyorffy, *Physical Review Letters* **28**, 801 (1972).
- [29] K. Terashima *et al.*, *Proceedings of the National Academy of Sciences* **106**, 7330 (2009).
- [30] E. R. Margine and F. Giustino, *Physical Review B* **87**, 024505 (2013).
- [31] W. McMillan, *Physical Review* **167**, 331 (1968).
- [32] P. B. Allen and R. C. Dynes, *Physical Review B* **12**, 905 (1975).
- [33] S. Haastrup *et al.*, *2D Materials* **5**, 042002 (2018).
- [34] M. N. Gjerding *et al.*, *2D Materials* **8**, 044002 (2021).
- [35] J. Noffsinger, F. Giustino, B. D. Malone, C.-H. Park, S. G. Louie, and M. L. Cohen, *Computer Physics Communications* **181**, 2140 (2010).
- [36] S. Poncé, E. R. Margine, C. Verdi, and F. Giustino, *Computer Physics Communications* **209**, 116 (2016).
- [37] H. Lee *et al.*, *npj Computational Materials* **9**, 156 (2023).
- [38] P. Giannozzi *et al.*, *Journal of physics: Condensed matter* **21**, 395502 (2009).
- [39] P. Giannozzi *et al.*, *Journal of physics: Condensed matter* **29**, 465901 (2017).
- [40] D. Hamann, *Physical Review B—Condensed Matter and Materials Physics* **88**, 085117 (2013).
- [41] T. Sohler, M. Calandra, and F. Mauri, *Physical Review B* **96**, 075448 (2017).
- [42] V. Kamysbayev, A. S. Filatov, H. Hu, X. Rui, F. Lagunas, D. Wang, R. F. Klie, and D. V. Talapin, *Science* **369**, 979 (2020).
- [43] S.-Y. Wang *et al.*, *The Journal of Physical Chemistry C* **126**, 3727 (2022).
- [44] J. Bekaert, C. Sevik, and M. V. Milošević, *Nanoscale* **14**, 9918 (2022).
- [45] X.-Z. Yin, H. Wang, Q.-H. Wang, N. Jiao, M.-Y. Ni, M.-M. Zheng, H.-Y. Lu, and P. Zhang, *Chinese Physics Letters* **40**, 097404 (2023).
- [46] M. Downes, C. E. Shuck, B. McBride, J. Busa, and Y. Gogotsi, *Nature protocols*, 1 (2024).
- [47] P. Urbankowski *et al.*, *Nanoscale* **8**, 11385 (2016).

- [48] L. Li, Z. Chen, Y. Hu, X. Wang, T. Zhang, W. Chen, and Q. Wang, *Journal of the American Chemical Society* **135**, 1213 (2013).
- [49] X.-H. Ma, K.-H. Cho, and Y.-M. Sung, *CrystEngComm* **16**, 5080 (2014).
- [50] Y. Ma, Y. Jing, and T. Heine, *2D Materials* **4**, 025111 (2017).
- [51] A. Puthirath Balan *et al.*, *Nature Nanotechnology* **13**, 602 (2018).
- [52] R. Friedrich, M. Ghorbani-Asl, S. Curtarolo, and A. V. Krasheninnikov, *Nano Letters* **22**, 989 (2022).
- [53] A. Padilha, M. Soares, E. Leite, and A. Fazzio, *The Journal of Physical Chemistry C* **123**, 16359 (2019).
- [54] J. P. Perdew and Y. Wang, *Physical Review B* **45**, 13244 (1992).
- [55] J. P. Perdew, K. Burke, and M. Ernzerhof, *Physical Review Letters* **77**, 3865 (1996).
- [56] L. Cheng, C. Zhang, and Y. Liu, *Physical Review Letters* **125**, 177701 (2020).
- [57] J. Bekaert, C. Sevik, and M. V. Milošević, *Nanoscale* **12**, 17354 (2020).
- [58] N. Jiao, H.-D. Liu, L. Yang, Y.-P. Li, M. Zheng, H.-Y. Lu, and P. Zhang, *Europhysics Letters* **138**, 46002 (2022).
- [59] Y. Zhang, J. Chen, J. Hao, M. Xu, and Y. Li, *Physical Review B* **110**, 064513 (2024).